International Journal of Advanced Engineering Research and Science (IJAERS)
Peer-Reviewed Journal
ISSN: 2349-6495(P) | 2456-1908(O)
Vol-13, Issue-3; Mar, 2026
Journal Home Page Available: https://ijaers.com/
Article DOI: https://dx.doi.org/10.22161/ijaers.133.5

Numerical Simulation Study on Internal Flow Field Characteristics of an Automotive ORC Piston Expander

Zi-Rui He, Yan-Zuo Chang*, Yong-Sen Huang, Hong-Rui Yang, Yu-Xuan Chen, Guan-Hong Xie, Jie-Zhen Yang, Kai-Ming Chen, Wen-Min Wen, Yong-Qing Wang

School of Energy and Power Engineering, Guangdong University of Petrochemical Technology, Maoming, Guangdong 525000, China
(Corresponding author: Yan-Zuo Chang), Email: 3435059931@qq.com

Received: 18 Feb 2026,

Received in revised form: 16 Mar 2026,

Accepted: 23 Mar 2026,

Available online: 29 Mar 2026

***Keywords*— ORC , Piston Expander, CFD, Internal Flow Field Characteristics, Clearance Height**

***Abstract*—** *Aiming at the problems of complex internal flow fields and the significant impact of clearance height on performance in Organic Rankine Cycle (ORC) waste heat recovery systems, this paper conducted a 3D steady-state numerical simulation study. Selecting the key working phase where the intake valve is fully open, a refined 3D model covering the intake port and the internal fluid domain of the cylinder was established, and ANSYS Fluent software was used for flow field analysis. The research results show that the computational model constructed in this paper has good convergence; after 5500 iterations, the energy residual reached the 10^{-7} level, and the residual curves of various physical quantities tended to be stable. This paper reveals the flow loss mechanism of the key phase of the expander, verifies the effectiveness of steady-state numerical simulation in evaluating the in-cylinder flow field characteristics, and provides theoretical support for further optimizing the intake structure and clearance height.*

I. INTRODUCTION

Against the macro-background of the increasingly severe global energy crisis and greenhouse effect, improving the thermal efficiency of internal combustion engines and achieving energy conservation and emission reduction in the transportation sector have become R&D priorities for the automotive industry. Statistical data show that only about 30% to 45% of the total heat released by fuel combustion in automotive diesel engines is converted into effective mechanical work, while as much as 35% of the energy is directly discharged into the atmosphere in the form of exhaust thermal energy [1,3].

To address the problems of low efficiency and serious heat waste in automotive internal combustion engines, the Organic Rankine Cycle (ORC) is widely recognized by academia and industry as an effective way to recover engine exhaust waste heat and improve vehicle fuel economy due to its excellent thermodynamic performance in medium-to-low grade heat recovery.[3,5]In an ORC system, the expander is the core executive component that converts the internal energy of the organic working fluid into mechanical energy, and its isentropic efficiency and volumetric efficiency directly determine the output power and thermodynamic performance of the entire waste heat recovery system. The selection of an expander typically depends heavily on specific application conditions. Compared to turbo-expanders (turbines), positive displacement expanders (such as piston and scroll types) possess physical characteristics like low rotational speed, high liquid slugging resistance, and large built-in expansion ratios, making them more suitable for automotive waste heat recovery scenarios with sharp fluctuations in exhaust energy.[2,4,6]

Currently, academic research on piston expanders mostly focuses on zero-dimensional or one-dimensional system-level simulations based on the lumped parameter method. While such studies can quickly predict the macro

power output of the system, they struggle to reveal the complex local flow field evolution and energy dissipation distribution within the cylinder. Existing literature points out that the clearance volume determined by the clearance height is the core geometric parameter restricting the volumetric efficiency of reciprocating machinery. At present, the microscopic mechanism of how clearance height affects intake jet structures, local throttling losses, and pressure energy transfer gradients under specific operating conditions still urgently needs in-depth analysis through high-precision 3D Computational Fluid Dynamics (CFD) methods. [9,10,11]

To address the limitations of existing research[6,7,8], this study adopts a 3D CFD simulation method targeting a piston expander under automotive exhaust conditions, selecting a typical intake phase to conduct steady-state numerical simulations and systematically analyzing its internal flow field characteristics. Specific tasks include: establishing a refined geometric model encompassing the intake port and in-cylinder clearance volume, and conducting local mesh refinement and mesh independence verification; analyzing the spatial distribution of the in-cylinder pressure field and throttling characteristics under a typical operating condition with an inlet total pressure of 1.0 MPa; and further evaluating the impact of flow field characteristics on the expander's work potential from a microscopic perspective, thereby providing data support for subsequent structural parameter optimization.

II. NUMERICAL SIMULATION METHOD AND MODEL ESTABLISHMENT

2.1 Establishment and Simplification of the Geometric Model

This paper focuses on a piston expander for automotive ORC systems. To improve numerical solving efficiency and ensure computational accuracy in core flow regions, the original 3D CAD model was physically simplified, extracting only the intake port, valve clearance, and the internal fluid domain of the cylinder, as shown in Figure 2. Based on a steady-state analysis strategy, this study extracts a representative key phase—"intake valve fully open with the piston near Top Dead Center"—for spatial modeling, aiming to explore the in-cylinder pressure buildup process and flow field distortion patterns during the initial intake stage.

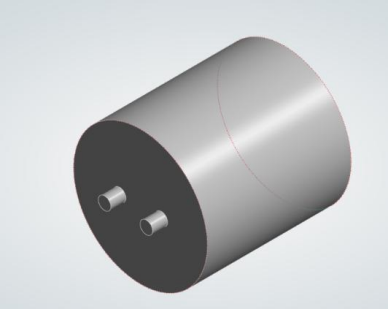

Fig.1： Physically simplified model

2.2 Governing Equations

The flow process of the organic working fluid within the cylinder involved in this paper follows the three classical conservation laws of fluid mechanics. Under a steady-state solver, its general governing equations are as follows:

Continuity Equation (Mass Conservation):

$$\frac{\partial}{\partial x_i}(\rho u_i) = 0 \qquad (1)$$

Momentum Conservation Equation (Navier-Stokes Equation):

$$\frac{\partial}{\partial x_j}(\rho u_i u_j) = -\frac{\partial p}{\partial x_i} + \frac{\partial \tau_{ij}}{\partial x_j} \qquad (2)$$

Energy Conservation Equation:

$$\frac{\partial}{\partial x_i}[u_i(\rho E + p)] = \frac{\partial}{\partial x_i}\left[k_{eff}\frac{\partial T}{\partial x_i}\right] \qquad (3)$$

Table 1 Nomenclature of physical quantities in the governing equations

Symbol	Description	Unit (SI)
ρ	Fluid density	kg/m^3
u_i, u_j	Velocity components in i, j directions	m/s
x_i, x_j	Cartesian coordinates	m
p	Static pressure	Pa
τ_{ij}	Viscous stress tensor	Pa
E	Total energy per unit mass	J/kg
k_{eff}	Effective thermal conductivity	$W/(m\cdot K)$
T	Thermodynamic temperature	K

2.3Mesh Generation and Independence Verification

Pre-processing software was used to perform unstructured mesh partitioning on the fluid domain. To accurately capture the jet morphology at the intake valve port, local mesh refinement was applied to the wall boundary layers and areas with abrupt changes in flow area.

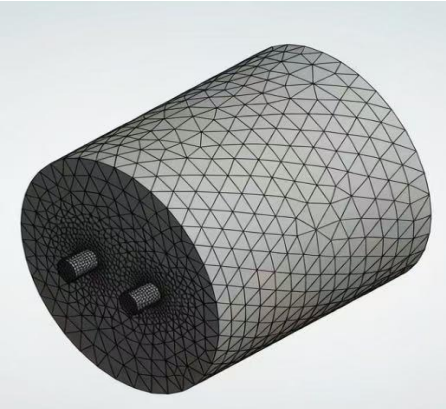

Fig.2: Mesh generation and independence verification of the fluid domain in the piston expander

To eliminate numerical interference caused by mesh size on the calculation results, three sets of mesh schemes with different densities were selected for independence verification. Using the static pressure value at the reference point in the center of the cylinder as the evaluation index, the results are shown in Table 2. Considering both computational accuracy and hardware resource overhead, Scheme 2 with approximately 1.2 million nodes was ultimately adopted for subsequent simulations.

Table 2 Grid Independence Verification Results

Grid Scheme	Grid Nodes (10^4)	Center point Static Pressure (MPa)	Relative Error
Scheme1(Coarse)	50	0.982	1.8%
Scheme2(Medium)	**120**	**1.001**	**Reference**
Scheme 3 (Fine)	240	1.003	0.2%

This paper conducted a grid independence verification using the static pressure value at the central characteristic point of the cylinder as the evaluation index, and its trade-off relationship is shown in Figure 3. Experimental data indicate that as the number of mesh nodes increased from 500,000 to 2.4 million, the calculated static pressure value gradually converged and stabilized within the range of 1.001–1.003 MPa.

From a logical analysis perspective, when the mesh scale doubled from 1.2 million (Scheme 2) to 2.4 million (Scheme 3), the relative fluctuation of the pressure value was only 0.2%. According to the relative error calculation formula, this fluctuation is far below the engineering allowable error range, proving that the calculation results have entered a convergence plateau within the restricted error range, and further mesh refinement has a minimal marginal contribution to calculation accuracy.

In summary, following the dual principles of grid independence and computational economy, this paper selected Scheme 2 (1.2 million nodes) as the numerical simulation baseline. This scheme successfully excludes the interference of discretization errors while achieving the optimal configuration of computational accuracy and efficiency, laying a reliable numerical foundation for subsequent flow field characteristic studies.

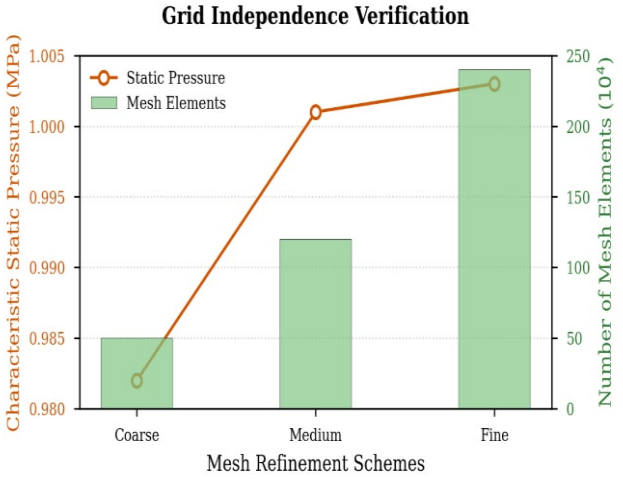

Fig.3: Impact of mesh density on computational accuracy and scale

2.4 Solver and Turbulence Model Settings

The simulation calculations were completed on the commercial fluid software ANSYS Fluent platform. A Pressure-Based Steady solver was employed. The standard k-ε model was selected as the turbulence model, which offers high engineering computational accuracy when handling confined flows near walls and jets with strong pressure gradients. The working fluid was set as R245fa, a commonly used organic fluid for ORC; its real thermodynamic property parameters, as shown in Table 2, were obtained through coupled calculations invoking the NIST standard database.

Table 3 Thermophysical properties and model settings of the working fluid

Parameter	Model / Value	Unit
Working fluid	R245fa	-
Density	Ideal gas / 400	kg / m^3
Specific heat C_p	1300	$J / (kg \cdot K)$
Thermal conductivity	0.08	$W / (m \cdot K)$
Dynamic viscosity	0.00018	$kg / (m \cdot s)$

2.5 Boundary Condition Settings

To accurately reflect the automotive exhaust energy recovery conditions, the following boundary conditions were set:

Inlet: A Pressure Inlet condition was adopted, with the total pressure set to 1.0 MPa.

Outlet: A Pressure Outlet condition was adopted; based on the system cycle condensation pressure, the backpressure was set to approximately 0.1 MPa.

Wall: The cylinder inner walls, intake port walls, and piston top surface were all set as adiabatic, No-slip solid wall boundaries.

III. SIMULATION RESULTS ANALYSIS AND DISCUSSION

Based on the numerical model and solver settings established in Chapter 2, this chapter analyzes the internal 3D steady flow field of the automotive ORC piston expander at the critical phase where the intake valve is fully open. First, the convergence of the computational process is evaluated to confirm the physical reliability of the obtained flow field data. Subsequently, the spatial distribution characteristics of the in-cylinder pressure field are systematically analyzed, focusing on clarifying the local throttling loss mechanism and the pressure buildup process within the clearance volume during intake. Finally, based on the steady-state flow field characteristics, the influence mechanism of clearance height on the expander's flow performance and work potential is deduced from a macroscopic perspective.

3.1 Computational Convergence and Reliability Analysis

The reliability of numerical simulation results heavily depends on the convergence of the computational process. In this study, key monitoring parameters such as residual curves of the governing equations and outlet mass flow rate were monitored in real-time in ANSYS Fluent to determine whether the flow field reached a statistical steady state.

As shown in Figure 4, after approximately 5500 iterations, the residual curves of all governing equations tended to be horizontal and dropped to extremely low levels.

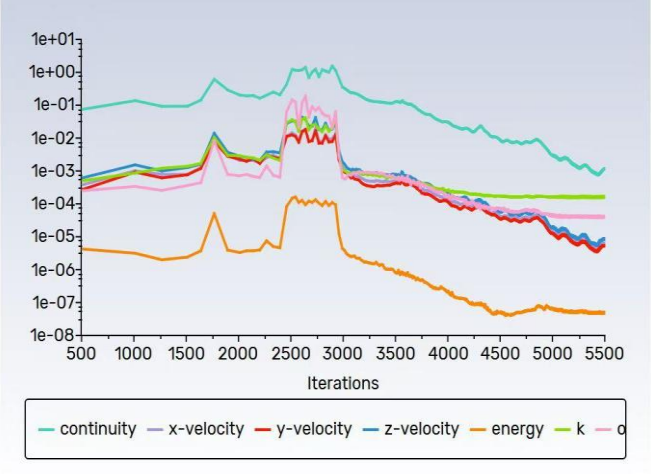

Fig.4: Numerical simulation residual convergence curves

Among them, the energy equation residual strictly converged to the 10^{-7} magnitude, while the momentum equation and continuity equation residuals stabilized at the 10^{-4} and 10^{-3} magnitudes, respectively. At the same time, the monitored mass flow rate at the outlet section tended to be constant in the later stages of iteration, with a fluctuation range of less than 0.1%. The deep convergence of the residuals and the stability of the monitoring parameters collectively indicate that the flow field has completely broken away from the transient influence of the initial state and reached a fully developed steady state. This ensures that the subsequently analyzed flow field structure and pressure distribution data are not products of numerical oscillation but steady-state solutions with clear physical meaning, laying a credible numerical foundation for subsequent flow field characteristic analysis.

3.2 In-cylinder Pressure Field Distribution and Throttling Characteristics

To reveal the flow details and energy conversion process of the working fluid during the initial intake stage, this section focuses on analyzing the distribution of the in-cylinder static pressure field. Figure 5 displays the static pressure cloud diagram on a horizontal section passing through the cylinder axis, clearly presenting a panoramic view of the high-pressure working fluid (R245fa) rushing in from the intake port and filling the clearance volume.

Figure 5 is a static pressure distribution cloud diagram of the cylinder's horizontal section (Top-down View) under the key intake phase of the expander. This

section clearly reveals the microscopic process of the high-pressure working fluid filling the clearance volume.

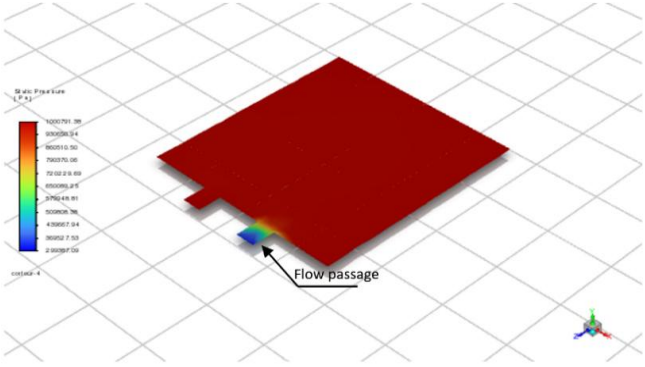

Fig.5: Static pressure distribution cloud diagram of the horizontal section in the cylinder

As can be seen from the pressure cloud diagram, when the high-pressure organic working fluid flows from the intake port into the cylinder, intense local flow resistance is triggered due to the sudden contraction of the flow passage cross-sectional area at the valve port. In this core region of the initial intake stage, a large amount of the fluid's static pressure energy is converted into kinetic energy, causing the pressure to plummet from the inlet's 1.0 MPa to a local low-pressure zone (approximately 0.3 MPa) behind the valve port. This distinct blue-green gradient area visually reflects the irreversible throttling loss of the piston expander during the intake process.

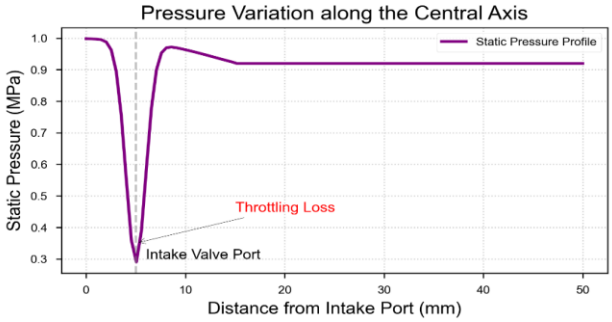

Fig.6: Pressure Variation along the Central Axis

To quantitatively evaluate the pressure loss during the intake process, a pressure distribution curve was extracted from the center of the intake port to the bottom of the cylinder, as shown in Figure 5. From the figure, it can be clearly observed that at the valve port position near the intake port, the pressure curve fluctuates violently, and the static pressure drops sharply to the lowest point, which corresponds to the local throttling zone in the cloud diagram. After entering the cylinder interior, as the flow passage cross-sectional area increases, the pressure rebounds significantly and eventually stabilizes at approximately 1.0 MPa. This process reveals the conversion characteristics between the fluid's kinetic energy and pressure energy.

The high-pressure jet passing through the valve port subsequently enters the clearance volume and rapidly diffuses to the surroundings inside the cylinder. As the flow area suddenly expands and the flow velocity decreases, the kinetic energy is converted back into static pressure energy (pressure recovery phenomenon). The cloud diagram shows that the pressure distribution gradient across the entire top space of the cylinder gradually becomes smooth, and the static pressure in most of the working areas stabilizes in the red high-value zone of the scale (approximately 1.0 MPa). This uniform and high-level initial backpressure distribution provides sufficient static pressure thrust for the impending downward expansion stroke of the piston.

3.3 Macroscopic Influence Mechanism of Clearance Height on Flow Field Characteristics

Based on the above steady-state flow field analysis, the macroscopic impact of the key geometric parameter, clearance height, on the expander's performance can be further deduced mechanistically.

Clearance height directly determines the distance between the intake valve port and the piston top surface, thereby dominating the development space of the intake jet. If the clearance height is too small, the intake valve port is too close to the piston top surface. At this time, the high-pressure jet directly impacts the piston surface before fully diffusing, which will lead to intense flow separation, vortex entrainment, and wall jets, significantly exacerbating the turbulent kinetic energy dissipation and pressure pulsation within the cylinder. Although a smaller clearance volume is beneficial for improving the theoretical volumetric efficiency, the excessive flow loss will severely weaken the effective pressure energy actually used for doing work.

Conversely, appropriately increasing the clearance height, although slightly increasing the "harmful" clearance volume and causing a slight drop in theoretical volumetric efficiency, provides crucial buffering and expansion space for the intake jet. As described in section 3.2.2, sufficient space allows the jet kinetic energy to convert into static pressure energy more smoothly, promoting pressure recovery and making the in-cylinder pressure distribution more uniform, thereby effectively reducing intake throttling loss and impact loss. Macroscopically, this manifests as an increase in the mean effective pressure within the cylinder.

Therefore, the design of clearance height is essentially seeking a balance between "flow loss" and "volumetric efficiency". An optimized clearance height should enable the working fluid to achieve efficient pressure recovery and momentum reorganization within the clearance volume, minimizing irreversible flow losses to the greatest extent possible under a controllable sacrifice of volumetric efficiency, thereby enhancing the overall work potential and isentropic efficiency of the expander. The steady-state flow field characteristics revealed in this study provide a clear physical picture and theoretical basis for the subsequent parametric optimization of the clearance height.

IV. CONCLUSION

3D steady-state computational model and meshing strategy established in this paper demonstrate excellent numerical stability; after 5500 iterations, the energy equation residual dropped to an extremely low level, verifying the high efficiency and accuracy of steady-state CFD analysis in capturing the local internal flow field characteristics of the expander. Based on this, the analysis indicates: under a 1.0 MPa inlet total pressure, the working fluid experiences a clear throttling and pressure drop phenomenon due to the sudden change in flow area when flowing through the intake valve port, and intense conversion between static pressure energy and kinetic energy occurs, which constitutes the main source of irreversible losses during the expander's intake process; meanwhile, after entering the clearance volume, the high-pressure working fluid exhibits good pressure recovery and diffusion characteristics, forming a uniformly distributed high-pressure zone (approximately 1.0 MPa) at the top of the cylinder, thereby ensuring the work capacity during the initial expansion phase. Aiming at automotive waste heat recovery conditions, engineering optimization suggestions include focusing on smoothing and optimizing the chamfer and flow passage profile of the intake valve port in subsequent structural designs to suppress throttling losses, and it is necessary to comprehensively balance volumetric efficiency and flow dissipation to calibrate the optimal clearance height parameter.

ACKNOWLEDGEMENTS

This work was supported by the Research Funding of GDUPT, Research on Heat Transfer Enhancement of Heat Sink by Inverse Calculation Design Method (No. 2019rc074), Research on Intelligent Monitoring and Control Technology of Air Conditioning Noise Based on Quantitative Conjugate Gradient Method, the Innovation Fund for Energy and Power Engineering named "Photovoltaic storage refrigeration clothing" (NO.20242C02) from the School of Energy and Power Engineering, Guangdong University of Petrochemical Technology, and Guangdong College Students' Innovation and Entrepreneurship Program in 2025 (Project No.: 25A015).

REFERENCES

[1] Li, X. N. (2014). Research on Design and Performance Optimization of Diesel Engine Waste Heat Recovery Bottoming System and Exhaust Heat Exchanger (Doctoral dissertation, Tianjin University).

[2] Yang, X. (2024). Development and Research an Oil-Free Linear Compressor for Miniature Refrigeration Systems (Master's thesis, University of Chinese Academy of Sciences, School of Engineering Science).

[3] Zhang, H. G., Zhao, R., Tian, Y. M., & Yang, Y. X. (2019). Development of Organic Rankine Cycle (ORC) Waste Heat Recovery for Vehicle Engines. *Journal of Beijing University of Technology*.

[4] Liu, S. W. (2024). Dynamic characterization and experimental study of scroll compressor reed valve (Master's thesis, Hefei University of Technology)

[5] Wang, X. F. (2016). Study on Reciprocating Piston Expander Waste Heat Recovery System Coupling ORC (Master's thesis, Jilin University).

[6] Liu, X. Y. (2023). Research on the Control Technology of Piston Balance Position Adjustment for Moving Coil Linear Compressor (Doctoral dissertation, Liaoning Technical University).

[7] Liu, T. (2025). Performance Study of High Power Valve Linear Compressor for Electric Vehicle Heat Pump Air Conditioning (Master's thesis, Yangzhou University).

[8] Du, Q. W., Liu, M., Yan, X., Zhang, Z., Zhang, C., Chen, X. A., ... & Liu, W. X. (in press). Investigation on Static Characteristics of Turbine Aerostatic Radial Bearing in Organic Rankine Cycle Matched with Micro Nuclear Reactor Power System. *Nuclear Power Engineering*, 1–10.

[9] Wang, X. Y., Jia, D. M., Li, Z. J., & Tian, H. X. (2020). Engineering application and optimization of combustion system for the large marine diesel engine. *Ship Science and Technology*, 42(7), 148–153.

[10] Lai, C. G., Chen, Y. Y., Wang, Y., Duan, M. H., & Zhou, Y. T. (2017). Numerical Simulation and Optimization Analysis of Combustion in a Diesel Engine. *Journal of Chongqing University of Technology (Natural Science)*, 31(6), 23–30.

[11] Duan, Y. L., & Hu, Y. H. (2013). Numerical simulation of pressure difference in cylinders of CZ60 /30 marine air compressor. *Computer Aided Engineering*, 22(1), 41–45+53.